The PRISMA Hand II: A Sensorized Robust Hand for Adaptive Grasp and In-Hand Manipulation

Huan Liu[1], Pasquale Ferrentino[1], Salvatore Pirozzi[2], Bruno Siciliano[1], and Fanny Ficuciello[1(✉)]

[1] University of Naples Federico II, Naples, Italy
`fanny.ficuciello@unina.it`
[2] University of Campania "Luigi Vanvitelli", Aversa, Italy

Abstract. Although substantial progresses have been made in building anthropomorphic robotic hands, lack of mechanical robustness, dexterity and force sensation still restrains wide adoption of robotic prostheses. This paper presents the design and preliminary evaluation of the PRISMA hand II, which is a mechanically robust anthropomorphic hand developed at the PRISMA Lab of University of Naples Federico II. The hand is highly underactuated, as the 19 finger joints are driven by three motors via elastic tendons. Nevertheless, the hand can performs not only adaptive grasps but also in-hand manipulation. The hand uses rolling contact joints, which is compliant in multiple directions. Force sensor are integrated to each fingertip in order to provide force feedback during grasping and manipulation. Preliminary experiments have been performed to evaluate the hand. Results show that the hand can perform various grasps and in-hand manipulation, while the structure can withstand severe disarticulation. This suggests that the proposed design can be a viable solution for robust and dexterous prosthetic hands.

Keywords: Underactuated hand · Grasping · Manipulation · Force sensor

1 Introduction

Substantial progresses have been made in building anthropomorphic prosthetic hands in the past two decades, using emerging technologies. Currently, there are several anthropomorphic hands available in the market, for example the Bebionic Hand (Ottobock GmbH.), the i-Limb Hand (Touch Bionics Ltd.) and the Brunel Hand (Openbionics Ltd.). Research results were also obtained in academia, including the prosthetic hands presented in [1–5].

However, one of the major complaints from prosthetic hand users is the lack of mechanical robustness [6,7], which leads to the rejection of the prosthesis. Repeated mechanical failure and the high cost of repair and replacement are the major reasons

of abandonment of upper-limb prostheses, as reported in [8]. Particularly, workers in labor-intensive or outdoor occupations do not frequently use robotic prostheses, since these hands are susceptible to damage during working [9].

To solve this problem, strong hand structure can be adopted to achieve a robust design. For example, the HERI II hand designed for humanoid robot is robust and adaptive to impacts when interacting with the objects and environment [10]. But for prosthetic hand application, bulky rigid parts maybe not suitable as they increase the weight of a hand. Moreover, from the point of view of anthropomorphism, a rigid-bodied robotic hand does not coincide with the distinguishing feature of human hand, which is inherently compliant.

Inspired by human hand, compliance has been introduced to robotic hands (mainly to the fingers) in different manners, to improve the robustness by absorbing external impact.

Elastic actuation have been introduced, for example series elastic tendon [11] and compliant link made from steel layers [12]. Elastic finger joints, including flexure-based [13,14] and spring-based [15] compliant joint were also attempted. The PISA/IIT Soft-Hand [1] using COmpliant Rolling-contact Elements (CORE) joint, are particularly interesting to our design.

In company with the progresses in soft robotics, fingers using continuum or soft structure were also designed. Spring-based continuum finger was used in robotic hand designs in [16,17], while soft fingers driven by compliant linkage mechanism [12], by pneumatic [18–20] and hydraulic power [21] were also proposed. Although soft material allows large deformation, concerns may still stem from the increased structural complexity and inadequate grasp force.

As the grasping capability of robotic hand is steadily improving and approaching human performance, one of the remaining gaps between human hand and prosthetic counterpart is dexterity, particularly in-hand manipulation dexterity. The capability of in-hand manipulation brings better accuracy, efficiency and also kinematic redundancy to the upper-limb, as observed from human upper-limb.

Recently developed fully-actuated hand, for example the Shadow Dexterous Hand (Shadow Robot Company LTD.), the KITECH hand [22] and the BCL-13 hand [20], have demonstrated some level of in-hand manipulation dexterity, benefiting from independently driven finger joints. However, it is challenging to integrate a large number of (usually over ten) actuators in an anthropomorphic design. Beside the difficulty on design, fully-actuated hand is also challenging in control, given that limited bandwidth of bio-signal interfaces can be utilized for control of prosthesis.

Underactuated hands have been proved efficient in grasping [1,2,13]. As less degree of actuation (DoA) is used to drive higher degree of freedom (DOF), the design of the hand can be largely simplified. Due to the adaptivity introduce buy the underactuation mechanism, the hand can adaptively grasp objects, without actively control every finger joint. Different underactuation mechanism, pulley, linkage, fluid, gears and continuum differential mechanism [23] have been attempt to design various hand designs.

Recently, underactuated hands have also been exploited for in-hand manipulation, by utilizing the elasticity of underactuated fingers [24]. Several robotic hands with in-hand manipulation capabilities have been introduced, including the iRobot-Harvard-Yale (iHY) hand [14], the GR2 gripper [25,26], the caging manipulation gripper [27],
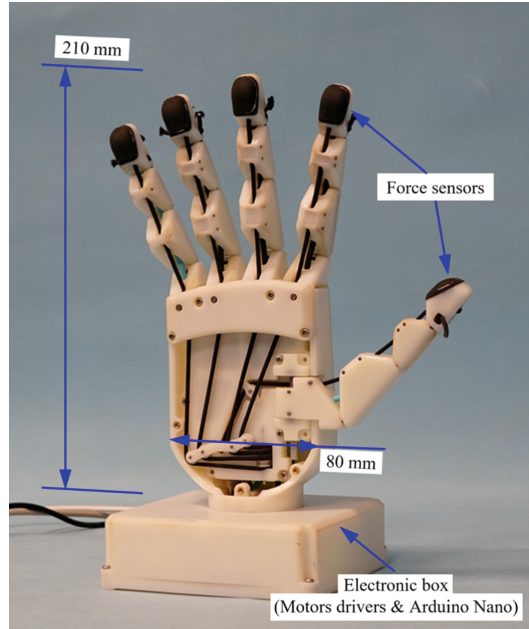
Fig. 1. The developed PRISMA hand II

the Pisa/IIT SoftHand 2 [28] and a single-actuator gripper in [29]. It can be seen from the above examples that underactuated hand can perform also in-hand manipulation if well designed.

Based on the research result obtained in [30], the PRISMA hand II was developed at the PRISMA (Projects of Industrial and Service Robotics, Mechatronics and Automation) Lab of the University of Naples Federico II, as shown in Fig. 1. The PRISMA hand II is a sensorized robust anthropomorphic hand, which has 19 joints driven by three motors. The length of the hand (measured from the tip of the middle finger to the wrist) is 210 mm, while the width of the palm is 80 mm. Underactuated transmission, different from the approach in [1,28], was adopted to achieve adaptive grasp and in-hand manipulation. Compliant rolling joints with notable compliance in multiple directions was implemented as finger joints of the hand. In addition, the hand has one force sensor on each of its five fingertip to provide grasp force feedback during grasping and in-hand manipulation. Experiments have verified that the hand can perform various adaptive grasps and also in-hand manipulation. Tests were also conducted to show that the hand can tolerate severe disarticulation, demonstrating the robustness of the design.

This paper is organized as follows. In Sect. 2, the underactuated design of the hand is presented. Section 3 describes the design and calibration of the sensors. Experimental characterizations are reported in Sect. 5 with the conclusions and future directions.

2 Underactuated Hand Design

This section presents the actuation strategy of the hand at first, followed by the design details of the adaptive fingers.
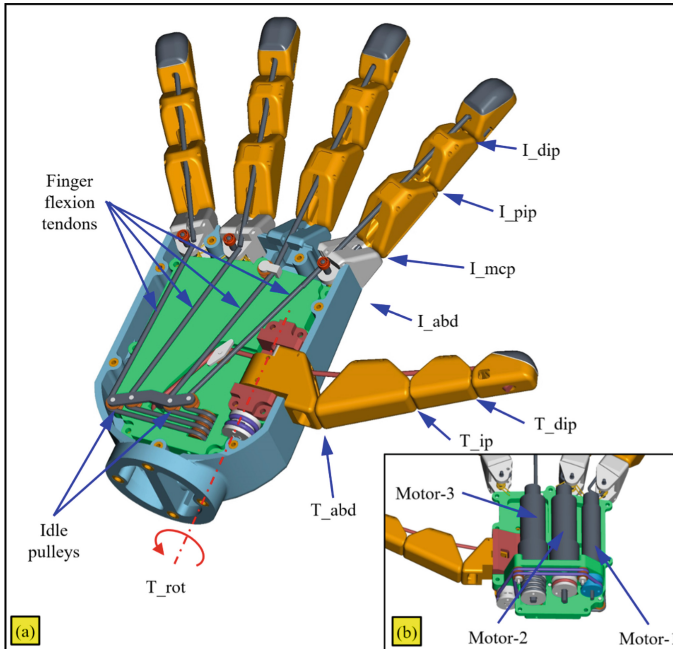
Fig. 2. Design of the hand: (a) The finger joints and tendon transmission of the hand. (b) The motors of the hand.

2.1 Actuation Strategy

The PRISMA hand II has 19 joints in total, as shown in Fig. 2(a). Each finger has four joints, except the middle finger that has only three. The thumb has three flexion/extension joints made from compliant rolling joints and one rotation joint which is a conventional revolute joint. Each of the index, the ring and the little finger has three compliant rolling flexion/extension joints and one revolute abduction/adduction joint. For the middle finger, the abduction/adduction joint is canceled. Letters T and I before the underscore indicate the joints for the thumb and the index finger respectively, as shown in Fig. 2. Abbreviations of rot, abd, mcp, ip, pip and dip indicate the rotation joint, the abduction/adduction joint, the metacarpophalangeal joint, the interphalangeal joint, the proximal and the distal interphalangeal joint, respectively.

The T_rot joint of the thumb is independently driven by Motor-1 (Maxon DCX12s 2.32W with 231:1 gearbox and ENX 10 EASY encoder) via two antagonistic tendons, as shown in Fig. 2(b). The tendons are elastic and preloaded, thus no extra pretensioner is needed. The three flexion joints (i.e. T_abd, T_ip and T_dip) of the thumb are driven by Motor-2 (Maxon DCX16s 7.91W with 231:1 gearbox and ENX 10 EASY encoder). The flexion of all fingers (except the thumb) were decided to be driven by Motor-3 (Maxon DCX16s 7.91W with 231:1 gearbox), as evidence showed strong correlation between flexion of all fingers [31]. Since the driving tendons are elastic, the fingers can adapt to grasped object therefore adaptive hand configuration can be formed.

Three Maxon motor drivers (EPOS2 24/2 530239), contained inside the electronic box shown in Fig. 1, receive motor position commands from a desktop and drive the motors accordingly.

The idea of using coordinated motions is inspired by the human hand. It is demonstrated to be the cornerstone towards smart hands simple to build and control while retaining much of the human hand functionality and skills [28, 32]. In general, the use of synergies creates a valid alternative that overcomes the limits of model-based methods for control and full-actuation trends for design [33–35].

Studies on fully actuated robotic hands demonstrate that thumb rotation depends especially from the third synergy that is responsible of successful precision grasps [36–40]. Considering the important role of the thumb on grasp stability, the rotation and flexion of the thumb are designed to be independently driven by Motor-1 and Motor-2, respectively. Although single-actuator hands (e.g. the Pisa/IIT hand [1] and hands with passive thumb rotation (e.g. the Bebionic V3 Hand and the hand in [2]) could perform various grasps, independent rotation and flexion of the thumb can further enhance grasp versatility and in-hand manipulation dexterity.

Underactuation based on compliant transmission has been used in robotic hand designs, for example in the TBM hand [41] and the Michlangelo Hand (Ottobock GmbH.). For actuation of the flexion of the fingers (except the thumb), the PRISMA hand II adopted a simpler design by using one motor to drive four elastic tendons of four fingers, as shown in Fig. 2(a). Therefore, no additional mechanism (e.g. spring, pulley or linkage) is needed. The PRISMA hand II is expected to have better robustness, benefiting from this structural simplicity.

2.2   Adaptive Finger Design

Compliant rolling contact joint [42] consists of a pair of surfaces in rolling contact with each other, with elastic elements holding them together. Several rolling joints were proposed, including the joints patented in [43, 44] and the joint used in the PISA/IIT SoftHand [1].

The PRISMA hand II adopted rolling contact joints as finger flexion joints. As shown in Fig. 3(a), each joint consists of a base link, a distal link, two ligaments and a tendon. The ligaments, made of elastic string, are attached to the base link and the distal link. The tendon, which is made from the same elastic string, is anchored to the distal link and threaded through the hole of the base link. At the extended configuration shown in Fig. 3(a), two facets of the links were held together by the elastic ligaments.

By pulling the tendon, the distal link is actuated and rolled on the cylindrical surface of the base link, as shown in Fig. 3(b). Once the driving tendon is released, the elastic ligaments return the distal link to the extended position, similar to a torsional spring in a conventional pin joint. The elastic tendon and ligaments bring the joint multi-directional compliance, by allowing various disarticulation, including backward bend, sideway bend, twist and dislocation.

In this research, the tendons and ligaments were made from low-cost elastic string with a diameter of 2.5 mm, which is originally for clothing industry. It composed of rubber strands forming a core, wrapped in polypropylene braided covering.
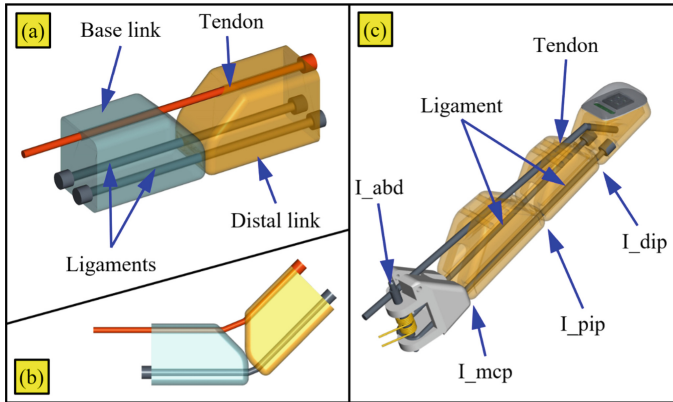
Fig. 3. The rolling contact joint in (a) extended configuration and (b) bent configuration. (c) Design of the index finger using the rolling contact joints.

The PRISMA hand II has five fingers with similar joint design, as each finger has one conventional revolute joint and three serially connected rolling contact joints driven by one elastic tendon. Take the index finger shown in 3(c) as an example, the I_abd, I_mcp, I_pip and I_dip joints are driven by one elastic tendon. When the driving tendon is pulled, the three rolling joints flex simultaneously. The structure parameters of the phalanges are designed to ensure the I_mcp joint flexes faster than the I_pip and the I_dip joint. Therefore the proximal phalanx will encounters an object first during power grasp. Then continuing to pull the tendon will close the I_pip and I_dip joints, thus conforming finger configuration can be formed. Finger parameters realizing such adaptive grasp can be found in [30].

3   Sensorization

This section introduces the design and calibration of the fingertip force sensor of the hand.

3.1   Sensing Principle

Recent progresses on sensor technology [45,46] enabled multiple force/tactile sensor solutions for robotic applications, including magnetic [47,48], capacitive [49,50], resistive [51,52] and optical [18,53–57]. Considering the limited space of the fingertip, a force sensing technology proposed in [58] based on optical components and deformable material was adopted. The method used multiple optical sensible points (called "taxels") to measure the deformation of the elastic layer over the points. After a calibration, the signals provided by the taxels can be used to estimate the force applied on the deformable layer.

The developed fingertip force sensor is shown in Fig. 4(a), with a one-EUR coin for reference. The fingertip measures 25 × 17 × 15 mm. As shown in Fig. 4(b), a printed
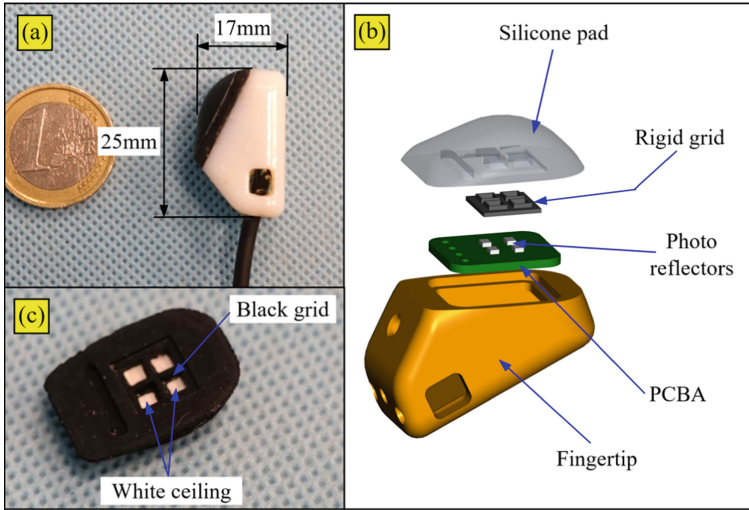
Fig. 4. The 3-axis force sensor of the PRISMA hand II. (a) The sensor dimensions. (b) The components of one sensor. (c) The deformable silicone pad.

circuit board assembly (PCBA) is installed inside a 3D-printed fingertip. On the PCBA, four photo reflectors (NJL5908AR by NJR Corporation, San Jose, CA, USA) are placed evenly with 3.4 mm separation. The photo reflector integrates the emitter and a receiver in the same package, which is an infrared Light Emitting Diode (LED), with a peak wavelength at 920 nm and a PhotoTransistor (PT), with a peak wavelength at 880 nm, respectively.

As an object is placed near a photo reflector, the voltage output of the receiver changes according to the distance between the object and the upper surface of the reflector. This relationship is non-monotonic according to the datasheet of the reflector. As the distance reduces, the voltage first goes up and reaches highest voltage at 0.25 mm distance. As the distance further decreases, the voltage drops. To avoid the non-monotonicity, a rigid 3D-printed grid is introduced between the PCBA and the silicone pad, to prevent the distance of reflection surface reaches 0.25 mm. The rigid grid is printed by black material to reduce crosstalk.

The silicone pad was cast using silicone molding technology. Figure 4(c) shows the bottom side of the pad, which has four cells to house the four photo reflectors. The walls are also black to reduce the crosstalk between taxels while the ceilings are white to facilitate reflection of infrared light. When an external force is applied on the silicone pad, the pad deforms and the distance between the white surface and the photo reflector changes. Therefore the intensity of the reflected light varies accordingly and the voltage output of the photo reflector changes.

An Arduino Nano and an Adafruit TCA9548A multiplexer, installed inside the electronic box shown in Fig. 1, were used to read the voltage change of the sensors and send to a desktop via serial connection.
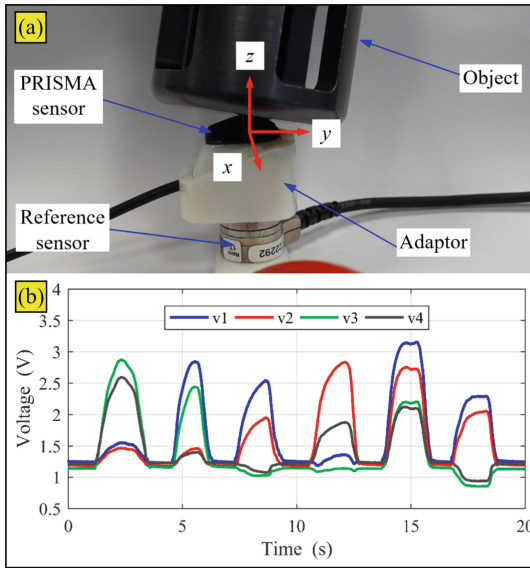
Fig. 5. (a) The setup for collecting data for sensor calibration. (b) 20 s of signal recorded from the four taxels of the sensor during data collection

3.2   Calibration

To calibrate the sensors, i.e. to obtain the relationship between applied force and voltage outputs of the photo reflector, sufficient data ($\approx$30000 pairs of force and voltage data) were collected and then neural network was adopted to learn the relationship.

Data were collected using the setup shown in Fig. 5(a). The developed fingertip is installed to a reference force sensor (ATI NANO 17 F/T Sensor) by an adapter. Then the silicone pad is pushed from various directions, using a flat surface of a rigid object. The force measurements of the reference sensor and the voltage signals of the PRISMA hand II sensor are both recorded, at a sample rate 180 Hz. For calibration of each fingertip sensor, about 180 s of measurement are recorded. Figure 5(b) shows 20 s of the voltage signals from the four taxels of the thumb. The voltage output of the taxels is about 1.2 V when no force is applied. When force is applied, the voltage rises.

The neural network is built and trained using the Neural Networks Toolbox in MATLAB. All of the networks for sensors have the same architecture, chosen experimentally and consisting of one hidden layer with ten neurons and one output layer with three neurons (corresponding to three directions of the contact force). The data of recorded force and voltage are randomly divided into training, validation, and test subsets comprising 70%, 15%, and 15%, respectively. The weights are randomly initialized using the Nguyen-Widrow rule, and the Levenberg-Marquadt algorithm is used for training.

Figure 6 (a), (b) and (c) shows the same 20 s of force measured by the Finger-1 sensor and the reference ATI sensor on the x-, y- and z-direction, respectively. As indicated
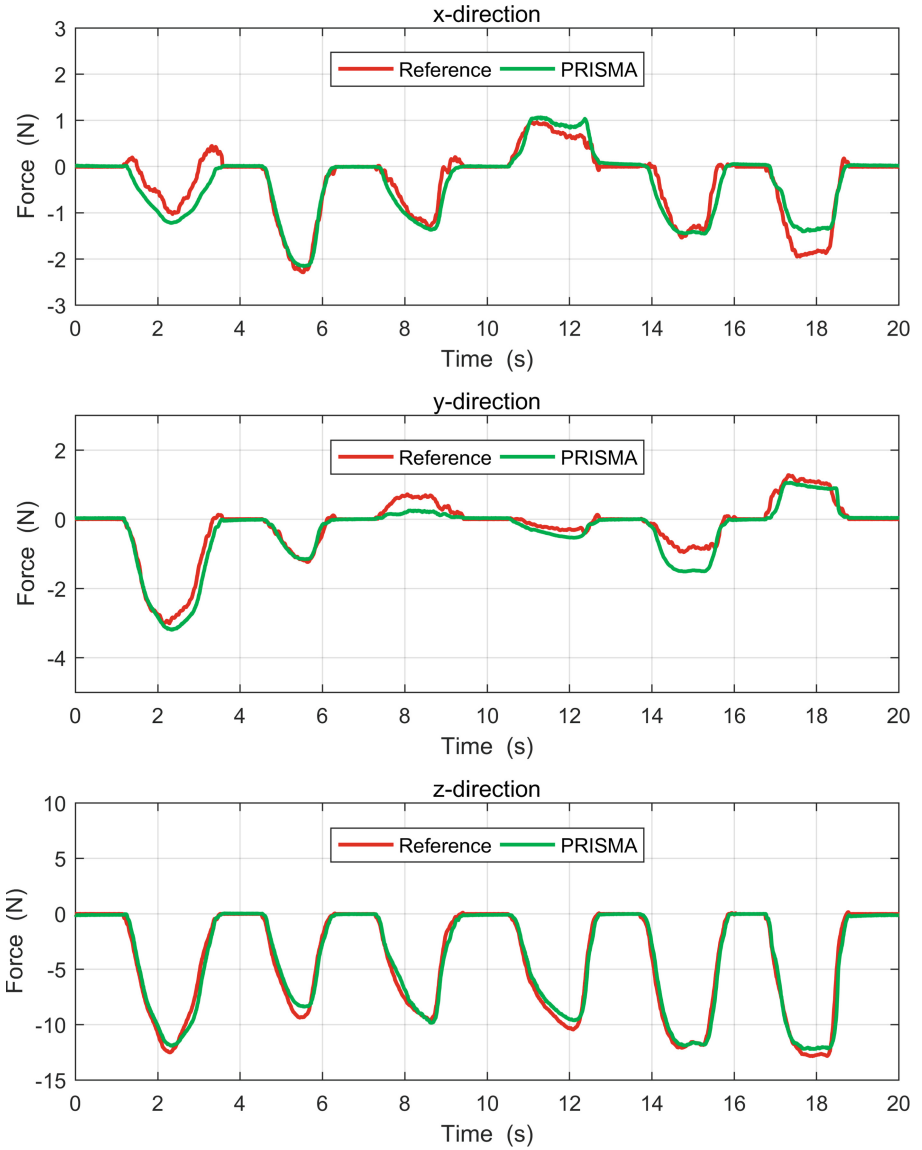
Fig. 6. The comparison of force measured by reference sensor and the developed PRISMA hand II sensor on (a) x-direction, (b) y-direction and (c) z-direction

by the calibration result, the sensor has better accuracy and larger range (about 12N) on normal direction.

4   Experiment

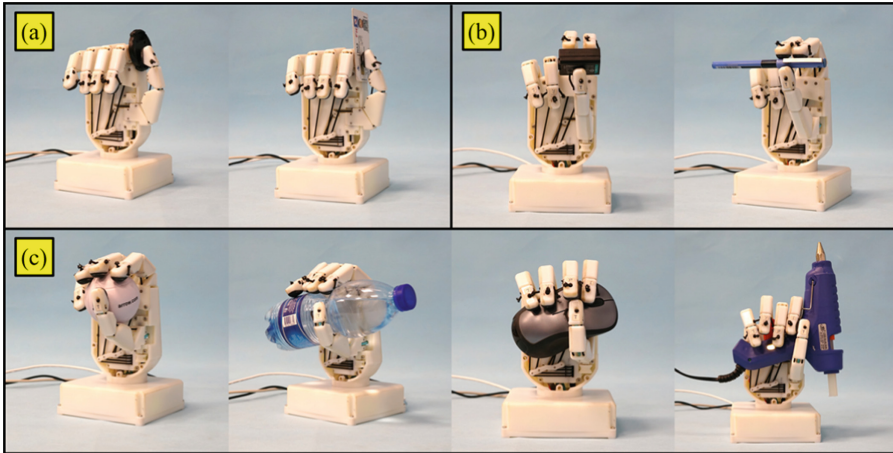This section presents preliminary experimentation of the PRISMA hand II.

Fig. 7. Grasping experiments: (a) power grasps, (b) pinches and (c) lateral grasps experiments

4.1 Grasping

To evaluate its grasping capability, the PRISMA hand II was commanded to grasp various objects. The hand could perform grasp patterns including lateral grasp, pinch grasp and power grasp, as shown in Fig. 7(a), (b) and (c), respectively.

For the lateral grasps shown in Fig. 7(a), the thumb was configured to the lateral position, the hand grasped the objects by the tip of the thumb and the lateral of the index finger. For the pinch and power grasps shown in Fig. 7(b) and (c), the thumb was at the position opposites the palm.

The contribution of the elastic tendon transmission is mostly notable in the pinch grasps shown in Fig. 7(b), as the hand is holding small objects with only the fingertips of the thumb, index and middle finger. When the index and middle finger were stopped by the object, the ring and little finger continued to flex until the adaptive grasp formed.

The fingers also adapted to different shapes of the objects, due to the underactuated finger design. Take the power grasps shown in Fig. 7(c) as examples, once the proximal phalanges were stopped by the object, continuing to pull the tendons closes the pip and then the dip joints, thus conforming finger configuration is formed.

4.2 In-Hand Manipulation

The PRISMA hand II was commanded to perform in-hand manipulation as shown in Fig. 8.

Figure 8(a) shows the manipulation of a ϕ60 mm foam ball using the thumb, index, middle and ring finger, while Fig. 8(b) shows the manipulation of and a ϕ50 mm plastic cup using the thumb, index and middle finger. The Motor-2 releases while Motor-3 pulls the tendons, thus the objects were move downward. Usually finger joints of a fully-actuated hand need to be coordinately controlled to maintain constant contact with
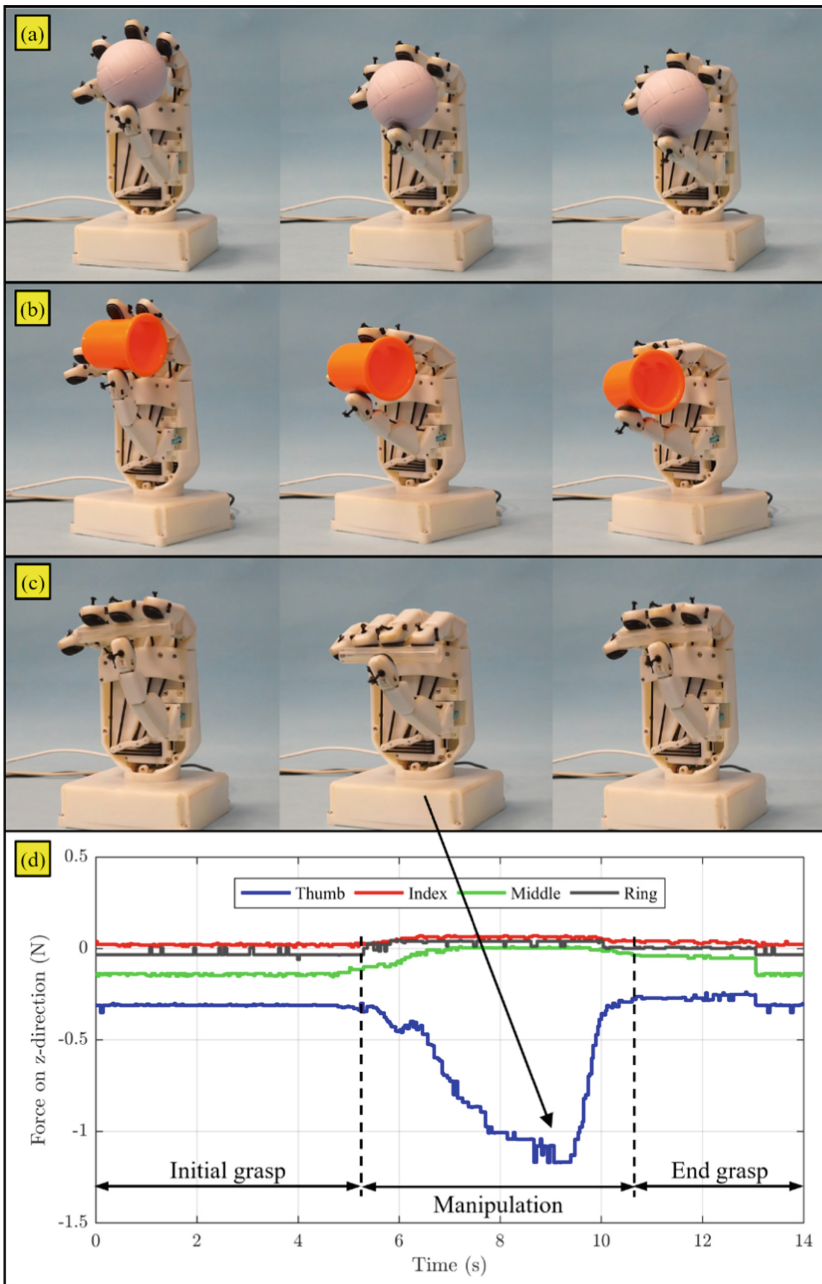
Fig. 8. The PRISMA hand II manipulating (a) a $\phi 60$ mm foam ball, (b) a $\phi 50$ mm plastic cup and (c) a $\phi 12$ mm cylinder. (d) The force recorded while manipulating the cylinder
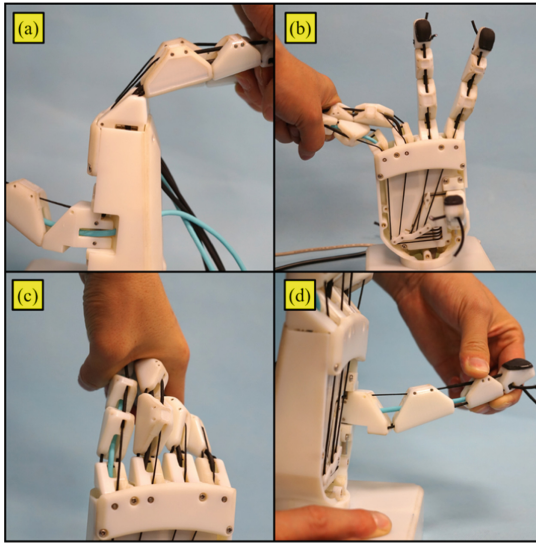
Fig. 9. Test of robustness of the PRISMA hand II. (a) Backward bend of the fingers. (b) Sideway bend of the ring and little finger. (c) Twist of the fingers. (d) Dislocation of the joints of the thumb.

an object, during in-hand manipulation. However, the compliant transmission based on elastic tendons of the PRISMA hand II alleviated the demand of complicated control.

Figure 8(c) shows the manipulation of a $\phi 12$ mm cylinder. The cylinder was rolled from the initial grasp configuration shown in the leftest photo, to the manipulation configuration shown in the middle photo and the end grasp configuration shown in the rightest photo. The normal force (z-direction) measured by the fingertip force sensors during the manipulation were recorded, as shown in Fig. 8(d). The force measured by the thumb sensor was the largest and changed most significantly, as the sensor opposites the index, the middle and the ring finger.

4.3   Test of Robustness

To verify the mechanical robustness of the PRISMA hand II, the fingers were intentionally disarticulated, including backward bend, sideway bend, twist and dislocation, as shown in Fig. 9(a)–(d), respectively. The phalanges restored their correct positions, after the removal of external force. The tests caused no damage to the joints or the elastic strings. As demonstrated by the tests, the fingers of the PRISMA hand II could withstand various deformation, due to the compliant joint design. This feature would be valuable when the hand is used in interaction with unstructured environment, for example being used as a prosthetic hand.

5   Conclusion and Future Work

Aiming at a sensorized robust anthropomorphic hand with adaptive grasp and in-hand manipulation capability, the PRISMA hand II was designed. Underactuation were

adopted thus the hand with 19 joints can be driven by only three motors. Compliant rolling contact joints were implemented as finger flexion joints, therefore the PRISMA hand II is robust to impact. In addition, force sensors based on optoelectronic technology were integrated to each fingertip to provide force feedback. Preliminary experiments showed that the hand could perform adaptive grasp and in-hand manipulation, while the fingertip sensors successfully provided contact force information. Additional test on robustness suggests that the proposed design might be a viable solution for robust and dexterous prosthetic hand.

Further investigation will be directed to a comprehensive study on in-hand manipulation using the PRISMA hand II, including deriving the manipulation primitives and exploring manipulation workspace of the hand. Standard protocol and more quantitative evaluation will be adopted to thoroughly assess the functionality of the hand. Control strategy utilizing contact force information will also be investigated, to achieve stable and precision manipulation of objects.

References

1. Catalano, M.G., Grioli, G., Farnioli, E., Serio, A., Piazza, C., Bicchi, A.: Adaptive synergies for the design and control of the Pisa/IIT SoftHand. Int. J. Robot. Res. **33**(5), 768–782 (2014)
2. Xu, K., Liu, H., Liu, Z., Du, Y., Zhu, X.: A single-actuator prosthetic hand using a continuum differential mechanism. In: 2015 IEEE International Conference on Robotics and Automation (ICRA), pp. 6457–6462. IEEE (2015)
3. Lenzi, T., Lipsey, J., Sensinger, J.W.: The RIC Arm—a small anthropomorphic transhumeral prosthesis. IEEE/ASME Trans. Mechatron. **21**(6), 2660–2671 (2016)
4. Controzzi, M., Clemente, F., Barone, D., Ghionzoli, A., Cipriani, C.: The SSSA-MyHand: a dexterous lightweight myoelectric hand prosthesis. IEEE Trans. Neural Syst. Rehabil. Eng. **25**(5), 459–468 (2017)
5. Xu, K., Liu, H., Zhang, Z., Zhu, X.: Wrist-powered partial hand prosthesis using a continuum whiffle tree mechanism: a case study. IEEE Trans. Neural Syst. Rehabil. Eng. **26**(3), 609–618 (2018)
6. Biddiss, E.A., Chau, T.T.: Upper limb prosthesis use and abandonment: a survey of the last 25 years. Prosthet. Orthot. Int. **31**(3), 236–257 (2007)
7. Østlie, K., Lesjø, I.M., Franklin, R.J., Garfelt, B., Skjeldal, O.H., Magnus, P.: Prosthesis rejection in acquired major upper-limb amputees: a population-based survey. Disabil. Rehabil. Assist. Technol. **7**(4), 294–303 (2012)
8. Bhaskaranand, K., Bhat, A.K., Acharya, K.N.: Prosthetic rehabilitation in traumatic upper limb amputees (an Indian perspective). Arch. Orthop. Trauma Surg. **123**(7), 363–366 (2003)
9. Cordella, F., et al.: Literature review on needs of upper limb prosthesis users. Front. Neurosci. **10**, 209 (2016)
10. Ren, Z., Kashiri, N., Zhou, C., Tsagarakis, N.G.: HERI II: a robust and flexible robotic hand based on modular finger design and under actuation principles. In: 2018 IEEE/RSJ International Conference on Intelligent Robots and Systems (IROS), pp. 1449–1455, October 2018

11. Grebenstein, M., et al.: The hand of the DLR hand arm system: designed for interaction. Int. J. Robot. Res. **31**(13), 1531–1555 (2012)
12. Choi, K.Y., Akhtar, A., Bretl, T.: A compliant four-bar linkage mechanism that makes the fingers of a prosthetic hand more impact resistant. In: 2017 IEEE International Conference on Robotics and Automation (ICRA), pp. 6694–6699. IEEE (2017)
13. Dollar, A.M., Howe, R.D.: The highly adaptive SDM hand: design and performance evaluation. Int. J. Robot. Res. **29**(5), 585–597 (2010)
14. Odhner, L.U., et al.: A compliant, underactuated hand for robust manipulation. Int. J. Robot. Res. **33**(5), 736–752 (2014)
15. Lotti, F., Tiezzi, P., Vassura, G., Biagiotti, L., Palli, G., Melchiorri, C.: Development of UB hand 3: early results. In: ICRA, pp. 4488–4493 (2005)
16. Potratz, J., Yang, J., Abdel-Malek, K., Pitarch, E.P., Grosland, N.: A light weight compliant hand mechanism with high degrees of freedom. J. Biomech. Eng. **127**(6), 934–945 (2005)
17. Makino, S., Kawaharazuka, K., Kawamura, M., Asano, Y., Okada, K., Inaba, M.: High-power, flexible, robust hand: development of musculoskeletal hand using machined springs and realization of self-weight supporting motion with humanoid. In: 2017 IEEE/RSJ International Conference on Intelligent Robots and Systems (IROS), pp. 1187–1192. IEEE (2017)
18. Zhao, H., O'Brien, K., Li, S., Shepherd, R.F.: Optoelectronically innervated soft prosthetic hand via stretchable optical waveguides. Sci. Robot. **1**(1), eaai7529 (2016)
19. Fras, J., Althoefer, K.: Soft biomimetic prosthetic hand: Design, manufacturing and preliminary examination. In: 2018 IEEE/RSJ International Conference on Intelligent Robots and Systems (IROS), pp. 1–6. IEEE (2018)
20. Zhou, J., Yi, J., Chen, X., Liu, Z., Wang, Z.: BCL-13: a 13-DOF soft robotic hand for dexterous grasping and in-hand manipulation. IEEE Robot. Autom. Lett. **3**(4), 3379–3386 (2018)
21. Schulz, S., Pylatiuk, C., Reischl, M., Martin, J., Mikut, R., Bretthauer, G.: A hydraulically driven multifunctional prosthetic hand. Robotica **23**(3), 293–299 (2005)
22. Lee, D.-H., Park, J.-H., Park, S.-W., Baeg, M.-H., Bae, J.-H.: KITECH-hand: a highly dexterous and modularized robotic hand. IEEE/ASME Trans. Mechatron. **22**(2), 876–887 (2017)
23. Xu, K., Liu, H.: Continuum differential mechanisms and their applications in gripper designs. IEEE Trans. Robot. **32**(3), 754–762 (2016)
24. Odhner, L.U., Dollar, A.M.: Stable, open-loop precision manipulation with underactuated hands. Int. J. Robot. Res. **34**(11), 1347–1360 (2015)
25. Rojas, N., Ma, R.R., Dollar, A.M.: The GR2 gripper: an underactuated hand for open-loop in-hand planar manipulation. IEEE Trans. Robot. **32**(3), 763–770 (2016)
26. Ward-Cherrier, B., Rojas, N., Lepora, N.F.: Model-free precise in-hand manipulation with a 3D-printed tactile gripper. IEEE Robot. Autom. Lett. **2**(4), 2056–2063 (2017)
27. Ma, R.R., Bircher, W.G., Dollar, A.M.: Toward robust, whole-hand caging manipulation with underactuated hands. In: 2017 IEEE International Conference on Robotics and Automation (ICRA), pp. 1336–1342. IEEE (2017)
28. Santina, C.D., Piazza, C., Grioli, G., Catalano, M.G., Bicchi, A.: Toward dexterous manipulation with augmented adaptive synergies: the Pisa/IIT SoftHand 2. IEEE Trans. Robot. **34**(5), 1141–1156 (2018)
29. Liu, H., Zhang, Z., Zhu, X., Xu, K.: A single-actuator gripper with a working mode switching mechanism for grasping and rolling manipulation. In: 2018 IEEE/ASME International Conference on Advanced Intelligent Mechatronics (AIM), pp. 359–364. IEEE (2018)
30. Liu, H., Xu, K., Siciliano, B., Ficuciello, F.: The mero hand: a mechanically robust anthropomorphic prosthetic hand using novel compliant rolling contact joint. In: 2019 IEEE/ASME International Conference on Advanced Intelligent Mechatronics (AIM). IEEE
31. Santello, M., Flanders, M., Soechting, J.F.: Postural hand synergies for tool use. J. Neurosci. **18**(23), 10105–10115 (1998)

32. Ficuciello, F., Federico, A., Lippiello, V., Siciliano, B.: Synergies evaluation of the SCHUNK S5FH for grasping control. In: Lenarčič, J., Merlet, J.P. (eds.) Advances in Robot Kinematics 2016. Springer Proceedings in Advanced Robotics, vol. 4, pp. 225–233. Springer, Cham (2018). https://doi.org/10.1007/978-3-319-56802-7_24

33. Ficuciello, F., Carloni, R., Visser, L., Stramigioli, S.: Port-Hamiltonian modeling for soft-finger manipulation. In: Proceedings of the IEEE/RSJ International Conference on Intelligent Robots and Systems, Taipei, Taiwan, pp. 4281–4286 (2010)

34. Ficuciello, F., Palli, G., Melchiorri, C., Siciliano, B.: Planning and control during reach to grasp using the three predominant UB Hand IV postural synergies. In: Proceedings of the IEEE International Conference on Robotics and Automation, Saint Paul, pp. 2255–2260 (2012)

35. Ficuciello, F., Zaccara, D., Siciliano, B.: Synergy-based policy improvement with path integrals for anthropomorphic hands. In: Proceedings of the IEEE International Conference on Intelligent Robots and Systems, Daejeon, Korea, pp. 1940–1945 (2016)

36. Gabiccini, M., Bicchi, A.: On the role of hand synergies in the optimal choice of grasping forces. In: Proceedings of Robotics: Science and Systems, Zaragoza (2010)

37. Ficuciello, F., Palli, G., Melchiorri, C., Siciliano, B.: A model-based strategy for mapping human grasps to robotic hands using synergies. In: Proceedings of the IEEE/ASME International Conference on Advanced Intelligent Mechatronics (AIM), Wollongong, Australia, pp. 1737–1742 (2013)

38. Ficuciello, F., Palli, G., Melchiorri, C., Siciliano, B.: Postural synergies and neural network for autonomous grasping: a tool for dextrous prosthetic and robotic hands. In: Pons, J., Torricelli, D., Pajaro, M. (eds.) Converging Clinical and Engineering Research on Neurorehabilitation. Biosystems & Biorobotics, vol. 1, pp. 467–480. Springer, Heidelberg (2013). https://doi.org/10.1007/978-3-642-34546-3_76

39. Ficuciello, F.: Synergy-based control of underactuated anthropomorphic hands. IEEE Trans. Ind. Inform. **15**, 1144–1152 (2019)

40. Cerulo, I., Ficuciello, F., Lippiello, V., Siciliano, B.: Teleoperation of the SCHUNK S5FH under-actuated anthropomorphic hand using human hand motion tracking. Robot. Auton. Syst. **89**, 75–84 (2017)

41. Dechev, N., Cleghorn, W., Naumann, S.: Multiple finger, passive adaptive grasp prosthetic hand. Mech. Mach. Theory **36**(10), 1157–1173 (2001)

42. Cannon, J.R., Lusk, C.P., Howell, L.L.: Compliant rolling-contact element mechanisms. In: ASME 2005 International Design Engineering Technical Conferences and Computers and Information in Engineering Conference, pp. 3–13. American Society of Mechanical Engineers (2005)

43. Hillberry, B.M., Hall Jr., A.S.: Rolling contact joint, 13 January 1976. US Patent 3,932,045

44. Ruoff, C.F.: Rolling contact robot joint, 17 December 1985. US Patent 4,558,911

45. Bartolozzi, C., Natale, L., Nori, F., Metta, G.: Robots with a sense of touch. Nat. Mater. **15**(9), 921 (2016)

46. Wang, H., Totaro, M., Beccai, L.: Toward perceptive soft robots: progress and challenges. Adv. Sci. **5**(9), 1800541 (2018)

47. Jamone, L., Natale, L., Metta, G., Sandini, G.: Highly sensitive soft tactile sensors for an anthropomorphic robotic hand. IEEE Sens. J. **15**(8), pp. 4226–4233 (2015). Inductive

48. Wang, H., Totaro, M., Blandin, A.A., Beccai, L.: A wireless inductive sensing technology for soft pneumatic actuators using magnetorheological elastomers. In: 2019 2nd IEEE International Conference on Soft Robotics (RoboSoft), pp. 242–248. IEEE (2019)

49. Schmitz, A., Maggiali, M., Randazzo, M., Natale, L., Metta, G.: A prototype fingertip with high spatial resolution pressure sensing for the robot iCub. In: Humanoids 2008 - 8th IEEE-RAS International Conference on Humanoid Robots, pp. 423–428 (2008). Capacitive

50. Maiolino, P., Maggiali, M., Cannata, G., Metta, G., Natale, L.: A flexible and robust large scale capacitive tactile system for robots. IEEE Sens. J. **13**(10), pp. 3910–3917 (2013). Capacitive

51. Chossat, J.-B., Park, Y.-L., Wood, R.J., Duchaine, V.: A soft strain sensor based on ionic and metal liquids. IEEE Sens. J. **13**(9), 3405–3414 (2013)

52. Zhang, T., Jiang, L., Liu, H.: Design and functional evaluation of a dexterous myoelectric hand prosthesis with biomimetic tactile sensor. IEEE Trans. Neural Syst. Rehabil. Eng. **26**(7), 1391–1399 (2018)

53. Puangmali, P., Althoefer, K., Seneviratne, L.D.: Mathematical modeling of intensity-modulated bent-tip optical fiber displacement sensors. IEEE Trans. Instrum. Meas. **59**(2), 283–291 (2009)

54. Noh, Y., Bimbo, J., Sareh, S., Wurdemann, H., Fraś, J., Chathuranga, D., Liu, H., Housden, J., Althoefer, K., Rhode, K.: Multi-axis force/torque sensor based on simply-supported beam and optoelectronics. Sensors **16**(11), 1936 (2016)

55. Xie, H., Jiang, A., Wurdemann, H.A., Liu, H., Seneviratne, L.D., Althoefer, K.: Magnetic resonance-compatible tactile force sensor using fiber optics and vision sensor. IEEE Sens. J. **14**(3), 829–838 (2013)

56. Polygerinos, P., Seneviratne, L.D., Althoefer, K.: Modeling of light intensity-modulated fiber-optic displacement sensors. IEEE Trans. Instrum. Meas. **60**(4), 1408–1415 (2010)

57. Costanzo, M., De Maria, G., Natale, C., Pirozzi, S.: Design and calibration of a force/tactile sensor for dexterous manipulation. Sensors **19**(4), 966 (2019)

58. De Maria, G., Natale, C., Pirozzi, S.: Force/tactile sensor for robotic applications. Sens. Actuators A Phys. **175**, 60–72 (2012). Optoelectric